Title

Sustained activation of guanylate cyclase-A with TDT, a natriuretic peptide derivative, exhibits cardiorenal protection in Dahl salt-sensitive hypertensive rats

Authors

Shohei Oishi, Naoko Suzuki, Yuri Hasui, Tsuyoshi Homma, Masanori Obana, Takahiro Nagayama, Yasushi Fujio

Laboratory of Clinical Science and Biomedicine, Graduate School of Pharmaceutical Sciences, Osaka University, Osaka, Japan (S.O., M.O., Y.F.)

End-Organ Disease Laboratories, Daiichi Sankyo Co., Ltd, Tokyo, Japan (S.O., Y.H., T.H.)

Rare Disease & LCM Laboratories, Daiichi Sankyo Co., Ltd, Tokyo, Japan (T.N.)

Research Function, Daiichi Sankyo Co., Ltd, Tokyo, Japan (N.S.)

1

Running Title: Cardiorenal protection of TDT in Dahl hypertensive rats

Corresponding Author:

Yasushi Fujio

Laboratory of Clinical Science and Biomedicine, Graduate School of Pharmaceutical

Sciences, Osaka University, Osaka, Japan

1-6 Yamadaoka, Suita, Osaka, 565-0871, Japan

Tel.: +81 6 6879 8258; fax: +81 6 6879 8253

E-mail: fujio@phs.osaka-u.ac.jp

Number of Text pages: 30

Number of Tables: 3

Number of Figures: 7

Number of References: 23

Number of Words in Abstract: 235 words

Number of Words in Introduction: 441 words

Number of Words in Discussion: 822 words

Nonstandard abbreviations:

ANP, atrial natriuretic peptide; BNP, B-type natriuretic peptide; CKD, chronic kidney disease; DS, Dahl salt-sensitive hypertensive; GC-A, guanylate cyclase-A; HF, heart failure; HR, heart rate; NEP, neprilysin; PKG, protein kinase G; SBP, systolic blood pressure; UP, urinary protein.

Section assignment: Cardiovascular

Abstract

Heart failure often presents with prognosis-relevant impaired renal function. To investigate whether the chronic activation of guanylate cyclase-A (GC-A) protects both heart and kidney, we examined the effects of TDT, a neprilysin (NEP)-resistant natriuretic peptide (NP) derivative, on cardiac and renal dysfunction in Dahl salt-sensitive hypertensive rats (DS rats). Pretreatment with NEP or NEP inhibitor did not influence GC-A activation by TDT both *in vitro* and *in vivo*, resulting in a long-acting profile of TDT compared to native human atrial NP (hANP). The repeated administration of TDT to DS rats suppressed the progress of cardiac hypertrophy, systolic/diastolic dysfunction, and proteinuria in a dose-dependent manner. Compared with vehicle and hANP, salt diet-induced podocyte injury was reduced by TDT, analyzed by urinary podocalyxin concentration, renal expression of nephrin mRNA, and glomerular expression of desmin protein. Since glomerular TRPC6 plays detrimental roles in podocyte homeostasis, we examined the renal expression of TRPC6 in DS rats and found that salt diet upregulated the expression of TRPC6. Importantly, TRPC6 induction was significantly decreased in TDT treated rats, compared with vehicle and hANP. Consistently, in primary cultured podocytes from DS rats, TDT inhibited ATP-induced calcium influx, similar to TRPC inhibitor SKF96365. Finally, TDT-mediated protection of podocytes was abolished by PKG inhibitor KT5823. In conclusion, TDT treatment attenuated heart and kidney dysfunction, accompanied by podocyte protection through inhibition of TRPC6. Thus, long-acting NPs could be new avenues for treatment of heart failure.

Introduction

Heart failure (HF) is one of the major causes of death that approximately 26 million people suffer from worldwide (Ambrosy et al., 2014). Blockade of neurohumoral systems, such as the renin-angiotensin-aldosterone system (RAAS) and the sympathetic nervous system (SNS), improves the prognosis of the patients with HF significantly but its efficacy is still unsatisfactory. Patients with HF, especially those due to hypertension, have a high prevalence of prognosis-relevant comorbidities such as chronic kidney disease (CKD). Accumulating evidence has demonstrated that interaction between the heart and kidney bidirectionally accelerates the progression of their pathology, which is termed as cardiorenal syndrome (Schefold et al., 2016). Therefore, therapeutic strategies against HF should be considered not simply from the point of view of cardioprotection but also from renoprotection.

Natriuretic peptides (NPs), including atrial natriuretic peptide (ANP) and B-type natriuretic peptide (BNP), bind to their receptor guanylate cyclase-A (GC-A), thereby enhancing intracellular cGMP followed by activation of protein kinase G (PKG). NP/GC-A/cGMP/PKG cascade functions as a key regulator of body fluid and blood pressure, regulating multiple physiological outputs, such as natriuresis, vasodilation, and renin-angiotensin-aldosterone inhibition, and it is proposed that NPs play protective roles in cardiac and renal dysfunction (Volpe, 2014). In this context, carperitide, recombinant human ANP, is clinically used as a primary medication to treat acute heart failure (AHF) patients in Japan. Moreover, based on the evidence from preclinical experiments using genetically engineered animals (Kishimoto et al., 2009) and from population-based human studies (Seidelmann et al., 2017), it is theoretically proposed that chronic enhancement of blood NPs could improve prognosis in chronic heart failure (CHF) patients. However, in spite of the beneficial effects of treatment with NPs, chronic

treatment of native NPs is not practical due to their short half-lives because NPs are enzymatically degraded by neprilysin (NEP) (Hashimoto et al., 1994).

Recent peptide engineering technology has structurally modified native NPs to prolong their half-lives by conferring resistance to enzymatic degradation by NEP (Meems and Burnett, 2016).   In this study, TDT, an NEP-resistant derivative from taipan natriuretic peptide (TNP) (Alewood et al., 2008), was used to achieve sustained activation of GC-A. Considering that NEP inhibitor, in combination with angiotensin II receptor blocker, clinically improves the prognosis of CHF patients without worsening renal function (McMurray et al., 2014), it is likely that TDT could be a novel promising drug for CHF; however, its pharmacological characterization and medical benefits remain to be elucidated.

Here, we have hypothesized that sustained activation of GC-A could improve cardiac and renal disorders of HF due to hypertension.   And we examined the effects of sustained GC-A activation by TDT on cardiac and renal dysfunction using Dahl salt-sensitive hypertensive rats (DS rats).

5

JPET #244459

Materials and Methods

Peptides

TDT (SDSKIGNGCFGHKIDRINHVSNLGCNRIMQNPPKKFSGE, disulfide bond between C9-C25) was synthesized by Scrum Inc. (Tokyo, Japan) as described in Patent No. US2008015374 (Alewood et al., 2008). The purity was confirmed by HPLC analysis to be > 95%. hANP was purchased from Daiichi Sankyo Co., Ltd. (Tokyo, Japan).

Animals

All experimental procedures were approved by the Institutional Animal Care and Use Committee of Daiichi Sankyo Co., Ltd. The investigation conformed to the Guide for the Care and Use of Laboratory Animals, Eighth Edition, updated by the US National Research Council Committee in 2011.

In vitro human GC-A/cGMP assay

The open reading frame of human GC-A (hGC-A) constructed in vector pCMV6-Entry (Catalog No. RC209267) was purchased from OriGene Technologies, Inc. (Rockville, MD, USA). CHO-K1 cells were stably transfected with the plasmid DNA by Lipofectamine (Thermo Fisher Scientific, Waltham, MA, USA) and selected by G418 (Thermo Fisher Scientific) using a limiting-dilution method to obtain a single clone. CHO/hGC-A stable clones were then screened for the best response to hANP.

For the cGMP assay, hGC-A-expressing or parental CHO cells were seeded in a 384-well plate at 4×10^3 cells/well and cultured for 1 day under 5% CO_2 at 37 °C. After removal of culture medium, the cells were incubated with 1.6 mM 1-methyl-3-isobutylxanthine (Merck Millipore, Billerica, MA, USA) for 10 min followed

6

by incubation for 15 min with hANP or TDT which were pre-incubated with or without 10 µg/mL of NEP (R&D Systems, Minneapolis, MN, USA) for 30 min at 37 °C. The cells were lysed, and then cGMP concentration in the lysate was determined using a cGMP assay kit (Cisbio, Codolet, France).

In vivo plasma cGMP measurement

Plasma cGMP concentration was evaluated using 8-week-old male SD rats under isoflurane (2%) anesthesia. hANP or TDT at 100 nmol/kg was administrated via bolus injection just after intravenous infusion of saline or phosphoramidon (Santa Cruz Biotechnology, Dallas, TX, USA), a NEP inhibitor, at 825 nmol/kg/min for 2 min, followed by continuous administration at 165 nmol/kg/min until the end of the experiment according to a previous report (Hashimoto et al., 1994). cGMP concentration in Na_2EDTA plasma at each time point was measured by an EIA kit (GE Healthcare, Little Chalfont, UK).

Experimental protocol of chronic study

Male Dahl salt-sensitive (DS) rats were purchased from Japan SLC, Inc. (Shizuoka, Japan). The rats were maintained in a room at 50% relative humidity (acceptable range: 30% to 70%) and 22 °C (acceptable range: 19 °C to 25 °C) under a 12 h light/dark cycle, and allowed free access to diet (FR-2, Funabashi Farm, Chiba, Japan) and water.

At 7 weeks of age, rats started to be fed a high-salt diet (FR-2 containing 8% NaCl, Funabashi Farm) and at 12 weeks of age, divided into 4 groups (n = 13–14) based on body weight, systolic blood pressure (SBP), diastolic wall strain (DWS), left ventricular end-diastolic dimension (LVDd), and urinary protein (UP) excretion. The vehicle (5% glucose), hANP (40 nmol/kg), or TDT (low dose: 8 nmol/kg or high dose: 40 nmol/kg) was subcutaneously administrated twice a day for 8 weeks up to 20 weeks of age. As a

control, six rats were fed a normal-salt diet (FR-2 containing 0.3% NaCl).

Measurement of systolic blood pressure and heart rate

SBP and heart rate (HR) were measured by the tail-cuff method using a noninvasive sphygmomanometer (BP-98A, Softron, Tokyo, Japan) under conscious, restrained conditions at 11 (before dosing), 16, and 19 weeks of age. Individual data are presented as the mean values of three consecutive measurements.

Measurement of urinary and blood biochemical parameters

Twenty-four-hour urine collection and blood sampling were performed at 11 and 18 weeks of age. Urinary protein concentration and plasma creatinine concentration were measured by an automated clinical analyzer (BiOLiS 24i Premium; Tokyo Boeki Machinery, Tokyo, Japan) and urinary electrolytes were detected by an electrolyte analyzer (STAX-2; Techno Medica, Kanagawa, Japan). Urinary podocalyxin (Excocell, Philadelphia, PA, USA) and kidney injury molecule-1 (KIM-1, R&D systems) were determined by ELISA kits.

Echocardiography

High-resolution transthoracic echocardiography was performed using Vevo 2100 equipped with a 13-MHz linear array transducer (Fujifilm Visualsonics, Tronto, ON, Canada) under isoflurane (1.5-3%) anesthesia at 11 and 19 weeks of age, as described previously (Kumagai et al., 2016). Administration of test peptides was stopped on the day of the measurement. According to the method of Takeda et al. (Takeda et al., 2009), DWS was calculated as an indicator of myocardial wall stiffness using the parameters of LV posterior wall thickness at end-systole (LVPWs) and at end-diastole (LVPWd) using the following equation:

$$DWS = 1 - LVPWs / LVPWd$$

Hemodynamic measurements

The hemodynamic study was performed at 20 weeks of age under 2% isoflurane anesthesia using a catheter pressure transducer (Millar Instruments, Houston, TX, USA) according to a previously described method (Klotz et al., 2006). The time constant of LV isovolumic pressure decline, tau, was calculated using the Glantz method (Raff and Glantz, 1981).

Histopathological evaluation

The heart samples, fixed in 10% neutral buffered-formaldehyde solution, were embedded in paraffin. Sections were stained with hematoxylin-eosin (HE). Cross sectional areas of cardiomyocytes were measured by a researcher who was blinded to the experimental conditions, as the mean value of 100 eosin-positive cardiomyocytes of the papillary muscle using morphometric analysis software (analySIS; Soft Imaging System, Münster, Germany) in a randomly selected microscope field in each section.

Quantitative PCR

Relative gene expression in the kidney was determined by quantitative real-time polymerase chain reaction (PCR) using TaqMan Gene Expression Assays and TaqMan universal PCR master mix (Thermo Fisher Scientific) according to a general procedure (Arai et al., 2016). The following assays were used: B cell leukemia/lymphoma 2 (Bcl2; Rn99999125_m1), collagen 1a1 (Col1a1; Rn01463848_m1), interleukin-1β (IL-1b; Rn00580432_m1), nephrin (Nphs1; Rn00674268_m1), neutrophil gelatinase-associated lipocalin (NGAL; Lcn2; Rn00590612_m1), and glyceraldehyde-3-phosphate dehydrogenase (GAPDH; Rn99999916_s1). PCR

9

reactions were performed using a 7900 HT Fast Real Time PCR system (Thermo Fisher Scientific).   Relative mRNA levels of each gene were calculated by normalizing them to GAPDH mRNA level.

Glomerular protein expression

The kidney samples, fixed in 10% neutral buffered-formaldehyde solution, were embedded in paraffin and then sectioned.   Glomerular expression of TRPC6 and desmin was evaluated by semi-quantitative scoring of immunohistostained samples. Immunohistostaining was performed with an Envision+ kit (Agilent, Santa Clara, CA, USA) in accordance with the procedure described by the manufacturer.   Rabbit anti-rat TRPC6 (1:100 dilution; ACC-120; Alomone Labs., Jerusalem, Israel) and mouse anti-rat desmin (1:400 dilution; D33; Abcam, Cambridge, UK) antibodies were used as primary antibodies (Sonneveld et al., 2013) (Nijenhuis et al., 2011).   Glomerular TRPC6 and desmin expression was scored semi-quantitatively from 0 to 5 based on the extent of immunostaining intensity in 20 randomly-selected glomeruli per kidney (negative = 0, 1% to 20% positive with mild staining = 1, 1% to 20% positive with intense staining or 21% to 40% positive with mild staining = 2, 21% to 40% positive with intense staining or 41% to 60% positive with mild staining = 3, 41% to 60% positive with intense staining or 61% to 80% positive with mild staining = 4, and 61% to 100% positive with intense staining = 5).   Scoring was performed independently by two investigators who were blinded to the experimental conditions.

Primary cultured rat podocytes

Eighteen- to 21-week-old DS rats were fed an 8% NaCl containing diet from 7 weeks of age.   Podocytes were isolated according to the conventional sieving method (Chen et al., 2006) with minor modification.   In brief, renal cortical tissue homogenates were

strained through steel sieves with pore sizes in the order of 250, 150, and then 75 μm. The glomeruli retained on the top of the 75-μm sieve were washed and resuspended in ice-cold culture medium (DMEM/F-12 containing 5% fetal bovine serum supplemented with 0.5% Insulin-Transferrin-Selenium-A, and 100 U/mL penicillin-streptomycin). The glomeruli were then plated on collagen I-coated 10-cm dishes.   After 4 days culture in 5% CO_2 at 37 °C, outgrowing glomerular cells were trypsinized and passed over a 40-μm nylon strainer.   Only cells passing through the strainer were replated on collagen I-coated plates and cultured for 1 day.   The cultured cells mostly consisted of arborized or cobble stone-like podocytes under the light microscope.

Intracellular calcium measurements

Cultured rat podocytes, seeded at 3×10^4 cells/well in a 96-well plate for one day, were washed twice with PBS and then suspended in RPMI 1640 medium with or without 1 μM KT5823 (Merck Millipore), a PKG inhibitor, or 10 μM SKF96365 (Merck Millipore), a TRPC inhibitor.   Ninety minutes after the incubation, cells were treated with 10 μM Fura 2-AM (Thermo Fisher Scientific) and incubated for 30 min followed by wash and treatment with 100 nM TDT dissolved in Krebs-Ringer phosphate buffer (150 mM NaCl, 6 mM KCl, 1 mM $MgCl_2$, 10 mM D-glucose, and 10 mM HEPES) containing 1.5 mM $CaCl_2$ for 15 min.   The culture plates were mounted on an inverted microscope stage and exposed to 340 and 380 nm wavelength light using a multiple wavelengths high-solution fluorescence microscopy system (IonOptix, Westwood, MA, USA).   The arborized podocytes were then selected and monitored.   To stimulate calcium entry into the cells, 10 μM ATP (Merck Millipore) was added.   Data were presented as the fluorescence ratio 340 nm/380 nm.

Statistical analysis

Data are shown as means ± standard error (S.E.M.). Statistical analyses between two groups were performed by Student's or Welch's *t*-test. For multiple comparisons, the Dunnett's test or Tukey's test was performed depending on the purpose. Survival analysis was performed using Kaplan-Meier analysis and the log-rank test. A value of P < 0.05 was considered to be statistically significant. All statistical analyses were performed using SAS System Release 9.2 (SAS Institute, Tokyo, Japan).

Results

TDT activated GC-A in an NEP-resistant manner

To assess activation of GC-A by TDT, we measured the concentrations of cGMP in human GC-A (hGC-A)-expressing cells after stimulation with TDT or hANP (Fig. 1). TDT showed a full agonistic activity to hGC-A relative to hANP in a concentration-dependent manner, though the EC50 value of TDT was higher than that of hANP (TDT; 195 pM, hANP; 19 pM). Importantly, preincubation of hANP with NEP reduced hGC-A activation by hANP, but not that of TDT.

To evaluate the activation of GC-A with TDT *in vivo*, TDT or hANP was intravenously administered and plasma cGMP concentrations were measured. Plasma cGMP concentrations were more potently elevated and more slowly reduced by TDT than by hANP (Fig. 2A). Consistent with *in vitro* experiments, NEP inhibition by phosphoramidon enhanced AUC of cGMP after hANP administration up to a level similar to TDT alone, but did not significantly influence AUC after TDT treatment (Fig. 2B).

Chronic treatment of TDT ameliorated salt-induced hypertensive heart failure in DS rats

To address the beneficial therapeutic properties of TDT, DS rats were fed a high-salt diet and mortality, body weight, blood pressure, and heart rate were analyzed. Kaplan-Meier analyses revealed that the salt diet reduced the survival rate in DS rats and that mortality was improved by the treatment with TDT, compared to vehicle (Fig. 3A). In this experiment, we used two dosages of TDT and confirmed that TDT improved salt-induced mortality in a dose-dependent manner. Only one animal in 14 animals in TDT_low group died through the experiment while 6 /14 in Vehicle group. Considering

that TDT_high perfectly improved survival, TDT_low seemed to be effective, but statistical significance between TDT_low and Vehicle groups was not observed, probably because animals died concentratedly from 6 to 8 weeks in vehicle group. Consistent with the increased mortality, body weight gradually decreased in vehicle-treated rats, whereas body weight increased in TDT-treated animals with a significant difference at week 6 (Fig. 3B). Systolic blood pressure (SBP) was significantly elevated by the high-salt diet at the initiation of treatment with NPs, compared with control. Subsequent salt loading continued to elevate SBP comparably in vehicle, hANP, and TDT in the low-dosage (TDT_L) group, which was suppressed by TDT at high dosage (TDT_H) at week 4 (Fig. 3C). Compared with the control, the high-salt diet increased heart rate (HR) in the vehicle-treated group, but TDT significantly reduced HR at week 6 (Fig. 3D).

The high-salt diet induced cardiac hypertrophy with an increase of the left ventricle to body weight (LV/BW) ratio, which was reduced by TDT in a dose-dependent manner (Fig. 4A). Similarly, histological analyses demonstrated that the increase of cardiomyocyte size induced by the high-salt diet was reduced by hANP and TDT (Fig. 4C).

To examine the effects of TDT on cardiac function, echocardiographic analyses (Table 1) and hemodynamic assessments (Table 2) were performed. Echocardiographic examination demonstrated that the high-salt diet reduced fractional shortening (FS), ejection fraction (EF), stroke volume (SV), cardiac output (CO), and DWS, an indicator of ventricular wall stiffness, and that both TDT_L and TDT_H attenuated the impairment of these parameters. Consistently, hemodynamic analyses using a catheter showed that both systolic ($dP/dt_{max}/P$) and diastolic ($dP/dt_{min}/P$ and Tau) functions were deteriorated by the high-salt diet and that TDT ameliorated these functions. Of note, measurement by catheter method demonstrated that hANP and TDT at low dose did not lower BP,

14

while TDT at high dose significantly reduced BP, consistent with the data by tail cuff method.

TDT protected renal disorder induced by a high-salt diet in DS rats

Renal function was analyzed 6 weeks after NP treatment (Table 3). Urine protein (UP) excretion was increased in the high-salt diet groups compared to the normal-diet group at the initiation of NP therapy (data not shown). UP excretion progressively increased > 10 times in the vehicle group, compared with the control group. Importantly, TDT suppressed the increase in UP excretion induced by the high-salt diet. Though the sodium excretion/intake ratio was not influenced by NP treatment, each peptide potently enhanced creatinine clearance compared to the vehicle-treated group with statistical significance. To support these findings, we determined renal mRNA expression of inflammatory cytokine IL-1β, profibrotic marker Collagen 1a1, and anti-apoptotic marker Bcl-2. Salt overload up-regulated IL-1β and Collagen 1a1, and down-regulated Bcl-2, whereas hANP and TDT significantly inhibited these changes (Supplemental Figure).

Podocyte and tubular injury were suppressed by TDT

Given the anti-proteinuric effect of TDT, we next evaluated injury markers of tubules and podocytes, which play a pivotal role in the glomerular filtration barrier. Urinary Kim-1 excretion and mRNA expression of NGAL in the kidney were attenuated by TDT in a dose-dependent manner, indicating that hANP and TDT ameliorated tubular injury (Fig. 5A and B). Urinary excretion of podocalyxin, a component of the slit diaphragm in podocytes, was remarkably higher in the vehicle-treated group than in the control group, whereas both TDT_L and TDT_H, but not hANP, significantly suppressed the elevation (Fig. 5C). Consistently, mRNA expression of nephrin, an important component of the

15

renal filtration barrier, was upregulated by TDT in a dose dependent manner (Fig. 5D), while not by hANP.   Consistent with these results, immunohistological analyses using anti-desmin antibody demonstrated that glomerular desmin expression, an established podocyte injury marker, was less remarkable in the TDT-treated groups compared to the vehicle- and hANP-treated groups (Fig. 5E and F).   Taken together, TDT ameliorated both tubular and podocyte injury.   Since TDT more potently protected from podocyte injury than did hANP, and a recent report suggested that GC-A plays pivotal roles in podocyte homeostasis, we focused on the podocytes.

TDT reduced glomerular TRPC6 expression in a dose-dependent manner

To address the key renoprotective mechanism of TDT, we examined the glomerular protein expression level of TRPC6, since the upregulation of TRPC6 expression results in the impairment of podocyte homeostasis (Moller et al., 2007).   As depicted in Fig. 6, TDT reduced TRPC6 expression elevated by salt overloading in a dose-dependent manner.   Importantly, TDT_L exhibited inhibitory effects on TRPC6 induction more remarkably than hANP, suggesting that TDT could be a promising renoprotective drug.

   To examine whether TDT directly transduces its signals in podocytes, we stimulated cultured rat podocytes with TDT and measured cGMP production (Fig. 7A).   TDT stimulation promoted cGMP production, suggesting that TDT could preserve podocyte homeostasis directly.   Since TRPC6-mediated calcium influx deteriorates podocyte homeostasis (Winn et al., 2005), we tested the effect of TDT on intracellular calcium influx evoked by ATP with or without SKF96365 and KT5823 in primary rat podocytes (Fig. 7B and C).   Robust calcium influx induced by ATP was largely inhibited by pretreatment with SKF96365, a TRPC inhibitor, indicating that calcium influx was largely mediated by TRPC.   TDT reduced calcium influx and KT5823, a PKG inhibitor, completely abolished the effect of TDT, suggesting that TDT regulated TRPC function

16

through PKG.   Importantly the treatment with SKF96365 in combination with TDT did not exert additional inhibition compared with SKF96365 alone, indicating that TDT inhibited calcium influx mainly by inhibiting TRPC.

Discussion

HF is one of the major causes of death. Since the NEP inhibitor in combination with angiotensin receptor blocker improves the prognosis of HF, we hypothesized that NEP-resistant NPs could prevent HF progression. In the present study, we examined the effects of TDT, an NEP-resistant NP, on cardiac and renal dysfunction in DS rats. The repeated dosing of TDT ameliorated high-salt diet-induced cardiac hypertrophy and suppressed systolic and diastolic dysfunction. In addition to cardioprotective effects, TDT attenuated proteinuria induced by the high-salt diet. Moreover, TDT suppressed podocyte injury associated with the downregulation of TRPC6 expression. Interestingly, TDT directly activated GC-A and reduced calcium influx by inactivating TRPC6 activity in podocyte. Thus, we propose the protective effects of chronic treatment with NEP-resistant NPs as a long-acting GC-A activator against cardiac and renal disorders.

Entresto, a combination drug of the NEP inhibitor sacubitril and angiotensin receptor blocker valsartan, is clinically used as a novel anti-CHF drug to reduce the risk of cardiovascular death and hospitalization (McMurray et al., 2014). The cardioprotective effects of NEP inhibition are thought to be explained largely by the elevation of endogenous NPs (Solomon et al., 2012). However, since NEP inactivates a wide range of peptide hormones and secretory factors in addition to NPs (Campbell, 2017), it was difficult to make clear whether exogenous NP treatment could ameliorate CHF. Despite recent advances in peptide engineering technology and success in half-life extension of native NPs, there have been very few reports to reveal the therapeutic potential of their chronic application. Here, we focused on TDT as a novel NEP-resistant NP. TDT is an engineered NP derivative from taipan natriuretic peptide, which is isolated from the venom of the inland taipan (Alewood et al., 2008). Since TDT was resistant to degradation by NEP and exhibited cardiorenal protective effects, we could propose that

the NEP-resistant NP would be a novel therapeutic strategy, at least for HF patients intolerant of NEP inhibitors. In addition, considering that the upregulation of endogenous NPs by NEP inhibitor is theoretically limited, exogenous NPs could additionally activate GC-A. Further studies would be required to make clear whether TDT shows clinical benefits additive to NEP inhibitors.

Recent studies using genetically modified mice showed that podocyte-specific ablation of the NP receptor *GC-A* gene results in increased susceptibility to renal injury (Staffel et al., 2017), indicating that GC-A in podocytes plays important roles in renal protection; however, it remains to be fully elucidated whether pharmacological activation of the NP receptor protects kidneys from chronic stress, because conventional NPs are rapidly degraded by NEP. Here, using TDT, we successfully demonstrated that chronic activation of GC-A by long-acting NPs prevented renal dysfunction accompanied by protecting podocytes. Most importantly, TDT protected podocytes even at a low dose which didn't significant impact on blood pressure, glomerular filtration rate, and natriuresis. Considering the limitation of the dosing amount of GC-A activator due to its potent hypotensive effect, TDT could be a novel, well-balanced, renoprotective agent with regard to efficacy and safety.

However, to mention the direct organ protection of TDT, there are two major limitations in this study. First, the measuring methods of blood pressure, tail-cuff and intra-arterial catheter, could mask the changes in BP since animals were subjected to immorbilization and anesthetic stress. To assess chronic effect of TDT on BP in a condition closer to physiological settings, continuous recording of BP in free-moving animals would be needed. Second, it should be noted that our results, presented here, do not necessarily claim superiority of TDT over hANP, because hANP was used at a single dose. To compare the effectiveness of cardiac and renal protection between TDT and hANP adequately, it will be needed to analyze pharmacokinetic/pharmacodynamic

relationships using extra dosing amounts. In addition, we demonstrated that TDT protected not only podocytes but also tubules even at a low dose. Consistently, Kato et al. recently reported that systemic GC-A KO mice are more susceptible to renal damage than podocyte specific GC-A KO mice in a blood pressure-independent manner, which indicates the importance of other renal cells including tubules in the signaling of NPs (Kato et al., 2017). Further investigations regarding the direct protection of tubules by GC-A activation will be required.

Glomerulosclerosis is caused by NFAT-mediated induction of TRPC6 (Nijenhuis et al., 2011). As NFAT is activated by calcineurin in a calcium-dependent manner, it is likely that TRPC-mediated calcium influx induces TRPC6 expression as a positive feedback mechanism. In this context, it is important that TDT treatment reduced TRPC activity both *in vitro* and *in vivo*, contributing to the prevention of glomerulosclerosis. Interestingly, we also demonstrated that TRPC-mediated calcium influx was inhibited by PKG inhibitor, consistent with the previous report that the renal dysfunction by *GC-A* gene ablation is attenuated by a TRPC inhibitor (Staffel et al., 2017).

In conclusion, we demonstrated that TDT exhibited cardiorenal protection in DS rats. The generation of NEP-resistant NP using peptide engineering technology could be a promising strategy against cardiorenal diseases.

Acknowledgements

Authorship Contributions

Participated in research design: Oishi, Nagayama, and Fujio

Conducted experiments: Oishi, Suzuki, and Hasui

Performed data analysis: Oishi and Homma

Wrote or contributed to the writing of the manuscript: Oishi, Obana, and Fujio

References

Alewood P, Head GA and Fry BG (2008) Proteinaceous compounds and uses therefor. US patent US20080153747. 2008 Jun 26.

Ambrosy AP, Fonarow GC, Butler J, Chioncel O, Greene SJ, Vaduganathan M, Nodari S, Lam CS, Sato N, Shah AN and Gheorghiade M (2014) The global health and economic burden of hospitalizations for heart failure: lessons learned from hospitalized heart failure registries. *J Am Coll Cardiol* **63**:1123-1133.

Arai K, Morikawa Y, Ubukata N, Tsuruoka H and Homma T (2016) CS-3150, a Novel Nonsteroidal Mineralocorticoid Receptor Antagonist, Shows Preventive and Therapeutic Effects On Renal Injury in Deoxycorticosterone Acetate/Salt-Induced Hypertensive Rats. *J Pharmacol Exp Ther* **358**:548-557.

Campbell DJ (2017) Long-term neprilysin inhibition - implications for ARNIs. *Nat Rev Cardiol* **14**:171-186.

Chen CA, Hwang JC, Guh JY, Tsai JC and Chen HC (2006) TGF-beta1 and integrin synergistically facilitate the differentiation of rat podocytes by increasing alpha-smooth muscle actin expression. *Transl Res* **148**:134-141.

Hashimoto Y, Nakao K, Hama N, Imura H, Mori S, Yamaguchi M, Yasuhara M and Hori R (1994) Clearance mechanisms of atrial and brain natriuretic peptides in rats. *Pharm Res* **11**:60-64.

Kato Y, Mori K, Kasahara M, Osaki K, Ishii A, Mori KP, Toda N, Ohno S, Kuwabara T, Tokudome T, Kishimoto I, Saleem MA, Matsusaka T, Nakao K, Mukoyama M, Yanagita M and Yokoi H (2017) Natriuretic peptide receptor guanylyl cyclase-A pathway counteracts glomerular injury evoked by aldosterone through p38 mitogen-activated protein kinase inhibition. *Sci Rep* **7**:46624.

Kishimoto I, Tokudome T, Horio T, Garbers DL, Nakao K and Kangawa K (2009)

Natriuretic Peptide Signaling via Guanylyl Cyclase (GC)-A: An Endogenous Protective Mechanism of the Heart. *Curr Cardiol Rev* **5**:45-51.

Klotz S, Hay I, Zhang G, Maurer M, Wang J and Burkhoff D (2006) Development of heart failure in chronic hypertensive Dahl rats: focus on heart failure with preserved ejection fraction. *Hypertension* **47**:901-911.

Kumagai S, Nakayama H, Fujimoto M, Honda H, Serada S, Ishibashi-Ueda H, Kasai A, Obana M, Sakata Y, Sawa Y, Fujio Y and Naka T (2016) Myeloid cell-derived LRG attenuates adverse cardiac remodelling after myocardial infarction. *Cardiovasc Res* **109**:272-282.

McMurray JJ, Packer M, Desai AS, Gong J, Lefkowitz MP, Rizkala AR, Rouleau JL, Shi VC, Solomon SD, Swedberg K and Zile MR (2014) Angiotensin-neprilysin inhibition versus enalapril in heart failure. *N Engl J Med* **371**:993-1004.

Meems LMG and Burnett JC, Jr. (2016) Innovative Therapeutics: Designer Natriuretic Peptides. *JACC Basic Transl Sci* **1**:557-567.

Moller CC, Wei C, Altintas MM, Li J, Greka A, Ohse T, Pippin JW, Rastaldi MP, Wawersik S, Schiavi S, Henger A, Kretzler M, Shankland SJ and Reiser J (2007) Induction of TRPC6 channel in acquired forms of proteinuric kidney disease. *J Am Soc Nephrol* **18**:29-36.

Nijenhuis T, Sloan AJ, Hoenderop JG, Flesche J, van Goor H, Kistler AD, Bakker M, Bindels RJ, de Boer RA, Moller CC, Hamming I, Navis G, Wetzels JF, Berden JH, Reiser J, Faul C and van der Vlag J (2011) Angiotensin II contributes to podocyte injury by increasing TRPC6 expression via an NFAT-mediated positive feedback signaling pathway. *Am J Pathol* **179**:1719-1732.

Raff GL and Glantz SA (1981) Volume loading slows left ventricular isovolumic relaxation rate. Evidence of load-dependent relaxation in the intact dog heart. *Circ Res* **48**:813-824.

24

Schefold JC, Filippatos G, Hasenfuss G, Anker SD and von Haehling S (2016) Heart failure and kidney dysfunction: epidemiology, mechanisms and management. *Nat Rev Nephrol* **12**:610-623.

Seidelmann SB, Vardeny O, Claggett B, Yu B, Shah AM, Ballantyne CM, Selvin E, MacRae CA, Boerwinkle E and Solomon SD (2017) An NPPB Promoter Polymorphism Associated With Elevated N-Terminal pro-B-Type Natriuretic Peptide and Lower Blood Pressure, Hypertension, and Mortality. *J Am Heart Assoc* **6**.

Solomon SD, Zile M, Pieske B, Voors A, Shah A, Kraigher-Krainer E, Shi V, Bransford T, Takeuchi M, Gong J, Lefkowitz M, Packer M and McMurray JJ (2012) The angiotensin receptor neprilysin inhibitor LCZ696 in heart failure with preserved ejection fraction: a phase 2 double-blind randomised controlled trial. *Lancet* **380**:1387-1395.

Sonneveld R, Ferre S, Hoenderop JG, Dijkman HB, Berden JH, Bindels RJ, Wetzels JF, van der Vlag J and Nijenhuis T (2013) Vitamin D down-regulates TRPC6 expression in podocyte injury and proteinuric glomerular disease. *Am J Pathol* **182**:1196-1204.

Staffel J, Valletta D, Federlein A, Ehm K, Volkmann R, Fuchsl AM, Witzgall R, Kuhn M and Schweda F (2017) Natriuretic Peptide Receptor Guanylyl Cyclase-A in Podocytes is Renoprotective but Dispensable for Physiologic Renal Function. *J Am Soc Nephrol* **28**:260-277.

Takeda Y, Sakata Y, Higashimori M, Mano T, Nishio M, Ohtani T, Hori M, Masuyama T, Kaneko M and Yamamoto K (2009) Noninvasive assessment of wall distensibility with the evaluation of diastolic epicardial movement. *J Card Fail* **15**:68-77.

Volpe M (2014) Natriuretic peptides and cardio-renal disease. *Int J Cardiol* **176**:630-639.

Winn MP, Conlon PJ, Lynn KL, Farrington MK, Creazzo T, Hawkins AF, Daskalakis N, Kwan SY, Ebersviller S, Burchette JL, Pericak-Vance MA, Howell DN, Vance JM and Rosenberg PB (2005) A mutation in the TRPC6 cation channel causes familial focal segmental glomerulosclerosis. *Science* **308**:1801-1804.

Footnotes

Reprint requests to:

Shohei Oishi

End-Organ Disease Laboratories, Daiichi Sankyo Co., Ltd,

1-2-58 Hiromachi, Shinagawa-ku, Tokyo 140-8710, Japan

E-mail: oishi.shohei.pr@daiichisankyo.co.jp

Figure Legends

Fig. 1. TDT induces cGMP production via GC-A in an NEP-resistant manner.

CHO cells stably expressing human GC-A were incubated with the indicated concentrations of peptides for 15 min after pre-incubation with or without NEP for 30 min. cGMP concentrations were measured with an HTRF-based assay. Representative data are shown from three independent experiments that were performed in quadruplicate. Data are presented as the mean ± S.E.M. Error bars not shown are smaller than symbols.

Fig. 2. TDT administration enhances plasma cGMP concentration independently of NEP activity in rats.

(A) After bolus injection of TDT or hANP at 100 nmol/kg in the presence or absence of phosphoramidon, an NEP inhibitor (NEPi), plasma concentrations of cGMP were measured. (B) AUC of the change in plasma cGMP concentration from baseline is shown. Data are presented as the mean ± S.E.M (n = 3, each). $^{\$}P < 0.05$, $^{\$\$}P < 0.01$ vs. hANP -treated group.

Fig. 3. Effects of chronic TDT therapy on survival, body weight, systolic blood pressure, and heart rate in DS rats.

DS rats were fed a high-salt diet (8% NaCl) from 7 weeks of age. hANP or TDT was twice-daily subcutaneously dosed from 12 weeks of age for 8 weeks. Control: normal diet (0.3% NaCl)-fed group (n = 6). Vehicle: vehicle-treated group (n = 14). hANP: hANP (40 nmol/kg)-treated group (n = 14). TDT_L: TDT (8 nmol/kg)-treated group (n = 13). TDT_H: TDT (40 nmol/kg)-treated group (n = 13). (A) Survival rate. (B) Body weight. (C) SBP. (D) HR. Data are presented as the mean ± S.E.M. Error

bars not shown are smaller than symbols. † $P < 0.05$, ‡ $P < 0.01$ vs. Control, * $P < 0.05$, ** $P < 0.01$ vs. Vehicle.

Fig. 4. Chronic TDT therapy inhibited cardiac hypertrophy in DS rats.

Rats were fed a high-salt diet, concomitant with treatment of hANP or TDT.   (A) The left ventricular weight (LV)/body weight (BW) ratio was measured (n = 6 for Control, n = 13-14 for the other groups).   (B) Representative images of hematoxylin-eosin-stained sections of the left ventricle are shown (scale bar = 50 μm).   (C) Cross-sectional areas of cardiomyocytes were measured (n = 4 for Control, n = 8 for the other groups).   Data are presented as the mean ± S.E.M. ‡ $P < 0.01$ vs. Control, * $P < 0.05$, ** $P < 0.01$ vs. Vehicle.

Fig. 5. TDT, but not hANP, protected tubules and podocytes from high salt-induced injury in DS rats.

(A-B) Tubular injury markers and (C-F) podocyte injury markers were investigated. (A) Urinary excretion of KIM-1, an injury marker of proximal tubules, and (C) that of podocalyxin, an indicator of podocyte detachment and fragmentation, were measured at 18 weeks of age (n = 5 for Control, n = 10 for Vehicle, n = 11 for hANP, n = 12 for TDT_L, and n = 13 for TDT_H).   (B) mRNA expression of NGAL, another indicator of tubular injury, and (D) that of nephrin, a component of podocytes, were determined by real-time quantitative PCR in the DS rat kidneys at 20 weeks of age and normalized to the GAPDH mRNA level (n = 4 for Control, n = 8 for the other groups).   (E-F) Glomerular protein expression of the podocyte injury marker desmin was evaluated by immunohistochemical analysis.   (E) Representative images are shown (scale bar = 50 μm).   (F) Desmin protein expression was semi-quantitatively shown (n = 4 for Control, n = 8 for the other groups).   Data are presented as the mean ± S.E.M. ‡ $P < 0.01$ vs.

Control, $^{*}P < 0.05$, $^{**}P < 0.01$ vs. Vehicle or indicated group.

Fig. 6. TDT reduced glomerular expression of TRPC6 protein in DS rats.

Glomerular expression of TRPC6 protein in DS rats at 20 weeks of age was semi-quantitatively determined by immunohistochemical analysis. (A) Representative images are shown (scale bar = 50 μm). (B) Glomerular expression of TRPC6 protein was semi-quantitatively shown (n = 4 for Control, n = 8 for the other groups). Data are presented as the mean ± S.E.M. $^{‡}P < 0.01$ vs. Control, $^{**}P < 0.01$ vs. Vehicle or indicated group.

Fig. 7. TDT inhibited TRPC-mediated calcium influx through PKG in primary cultured rat podocytes.

(A) Primary cultured podocytes from DS rats were incubated with the indicated concentrations of TDT for 25 min. cGMP concentrations were then measured and normalized by protein amounts. Data are from four independent experiments performed in duplicate. (B-C) Cultured rat podocytes were pretreated with 100 nM TDT with or without TRPC inhibitor SKF96365 (10 μM) or PKG inhibitor KT5823 (1 μM) for 30 min, followed by exposure to 10 μM ATP to evoke Ca^{2+} influx. Intracellular Ca^{2+} concentration was determined by fura-2 ratiometry (n = 4-5). (B) Ca^{2+} influx was measured at the indicated time points. (C) AUC of the change in calcium influx from the baseline was calculated. Data are presented as the mean ± S.E.M. Error bars not shown are smaller than symbols. $^{*}P < 0.05$, $^{**}P < 0.01$ vs. Vehicle group, $^{\$\$}P < 0.01$ vs indicated group.

Table 1. TDT preserved cardiac systolic and diastolic function in DS rats.

Cardiac systolic/diastolic functional parameters were measured by echocardiography at 19 weeks of age (n = 6 for Control, n = 11 for Vehicle and hANP, n = 12 for TDT_L, and n = 13 for TDT_H).   Data are presented as the mean ± S.E.M. $^{\dagger} P < 0.05$, $^{\ddagger} P < 0.01$ vs. Control group, $^{*} P < 0.05$, $^{**} P < 0.01$ vs. Vehicle-treated group.   LVDd, left ventricular diameter in diastole; IVSd, intraventricular septum in diastole; LVPWd, left ventricular posterior wall in diastole; FS, fractional shortening; EF, ejection fraction; SV, stroke volume; CO, cardiac output; DWS, diastolic wall strain.

	Control	Vehicle	hANP	TDT_L	TDT_H
LVDd (mm)	7.50 ± 0.24	7.73 ± 0.31	7.88 ± 0.16	7.69 ± 0.21	7.84 ± 0.20
IVSd (mm)	2.16 ± 0.13	2.84 ± 0.08 ‡	2.59 ± 0.08 *	2.61 ± 0.08	2.35 ± 0.10 **
LVPWd (mm)	2.07 ± 0.09	2.62 ± 0.10 ‡	2.45 ± 0.05	2.55 ± 0.07	2.32 ± 0.05 *
FS (%)	41.0 ± 1.2	29.2 ± 3.3 †	34.9 ± 2.0	40.4 ± 2.5 **	44.8 ± 1.7 **
EF (%)	70.1 ± 1.5	53.0 ± 4.6 †	61.9 ± 2.9	68.6 ± 3.0 **	74.0 ± 1.9 **
SV (μl)	210 ± 14	161 ± 6 ‡	204 ± 8 **	214 ± 10 **	244 ± 13 **
CO (ml/min)	84.9 ± 5.3	62.4 ± 3.0 ‡	78.7 ± 3.1 **	81.6 ± 4.2 **	93.2 ± 4.9 **
DWS	0.328 ± 0.032	0.191 ± 0.021 ‡	0.262 ± 0.018	0.272 ± 0.017 **	0.348 ± 0.011 **

Table 2.   TDT improved hemodynamics in DS rats.

Hemodynamic parameters were measured by catheter with a pressure transducer at 20 weeks of age (n = 5 for Control, n = 7 for Vehicle, n = 6 for hANP, n = 9 for TDT_L, n = 9 for TDT_H).   Data are presented as the mean ± S.E.M.   [†] $P < 0.05$, [‡] $P < 0.01$ vs. Control group, [*] $P < 0.05$, [**] $P < 0.01$ vs. Vehicle-treated group.   SBP, systolic blood pressure; DBP, diastolic blood pressure; LVEDP, left ventricular end diastolic pressure.

	Control	Vehicle	hANP	TDT_L	TDT_H
SBP (mmHg)	138 ± 4	236 ± 3 [‡]	226 ± 5	227 ± 7	206 ± 6 [**]
DBP (mmHg)	97 ± 4	172 ± 2 [‡]	164 ± 4	165 ± 5	149 ± 5 [**]
dP/dt$_{max}$ (mmHg/sec)	8099 ± 402	10519 ± 767	9987 ± 451	12195 ± 714	11144 ± 625
dP/dt$_{max}$/P (/sec)	98.7 ± 3.0	78.2 ± 5.2 [†]	82.5 ± 2.5	92.9 ± 4.1 [*]	93.9 ± 1.9 [*]
dP/dt$_{min}$ (mmHg/sec)	-9706 ± 652	-9073 ± 582	-8971 ± 702	-10917 ± 511 [*]	-11594 ± 346 [**]
dP/dt$_{min}$/P (/sec)	-101.1 ± 4.4	-51.7 ± 4.1 [‡]	-59.6 ± 4.2	-68.5 ± 5.4 [*]	-76.9 ± 3.6 [**]
LVEDP (mmHg)	9.5 ± 1.1	13.1 ± 2.6	11.3 ± 1.5	10.0 ± 1.6	9.3 ± 1.5
Tau (msec)	12.0 ± 0.6	24.8 ± 3.8 [†]	20.2 ± 1.4	18.5 ± 1.4	16.3 ± 0.9 [*]

Table 3.   TDT improved renal function in DS rats.

Urine collection for 24 hours was performed at 18 weeks of age.   Data are presented as the mean ± S.E.M. $^{\dagger}P < 0.05$, $^{\ddagger}P < 0.01$ vs. Control group, $^{*}P < 0.05$, $^{**}P < 0.01$ vs. Vehicle-treated group.   UV, urine volume; UP, urinary protein; CCr, creatinine clearance.

	Control (n = 6)	Vehicle (n = 10)	hANP (n = 11)	TDT_L (n = 12)	TDT_H (n = 13)
UV (mL/day)	13.1 ± 3.0	95.9 ± 9.2 ‡	88.5 ± 8.6	76.5 ± 5.4	78.5 ± 5.7
Water intake (g/day)	35 ± 3	110 ± 9 ‡	105 ± 8	94 ± 6	96 ± 6
UP / day (mg/day)	27 ± 3	308 ± 32 ‡	277 ± 45	236 ± 32	190 ± 32 *
Na^{+} excretion / intake (g/g)	0.58 ± 0.09	0.31 ± 0.01 †	0.32 ± 0.01	0.33 ± 0.01	0.32 ± 0.01
CCr (mL/min)	2.0 ± 0.4	2.4 ± 0.3	3.5 ± 0.4 *	3.6 ± 0.3 *	4.2 ± 0.3 **

Fig. 1.

Fig. 2.

Fig. 3.

A

B

C

D

Fig. 4.

A

B

C

Fig. 5.

Fig. 6.

A

B

Fig. 7.

A

B

C
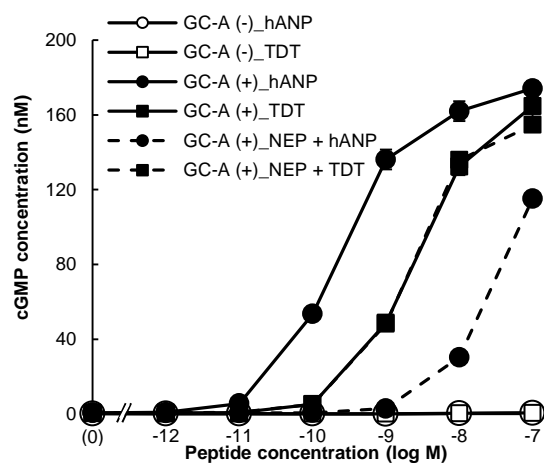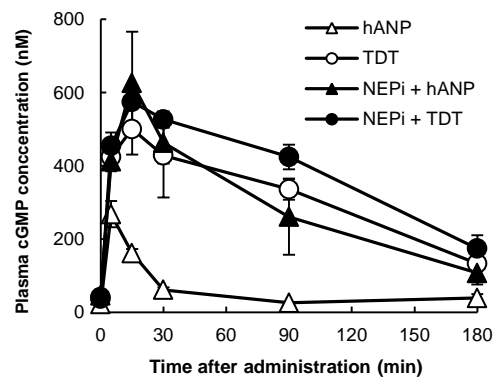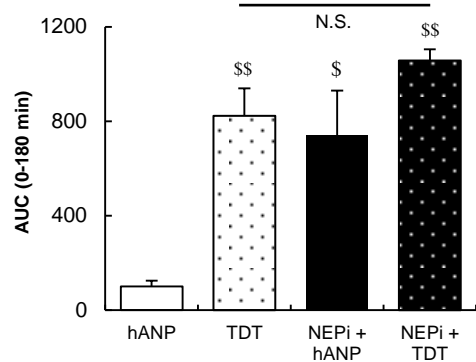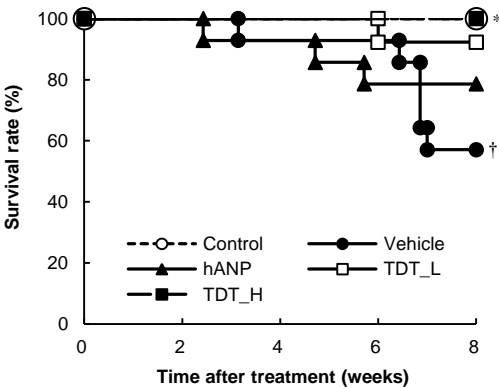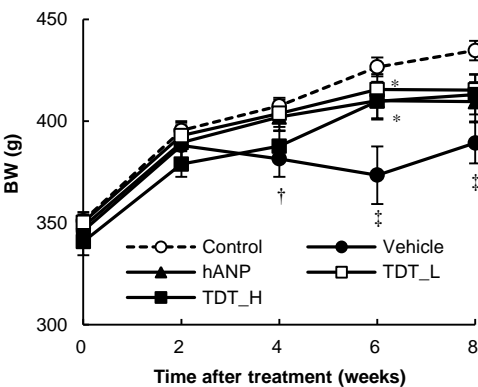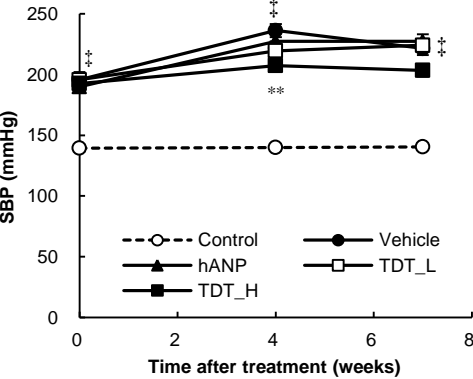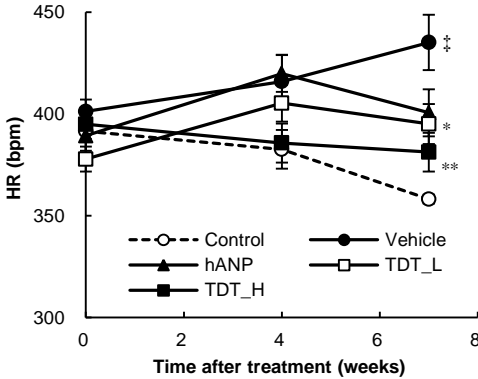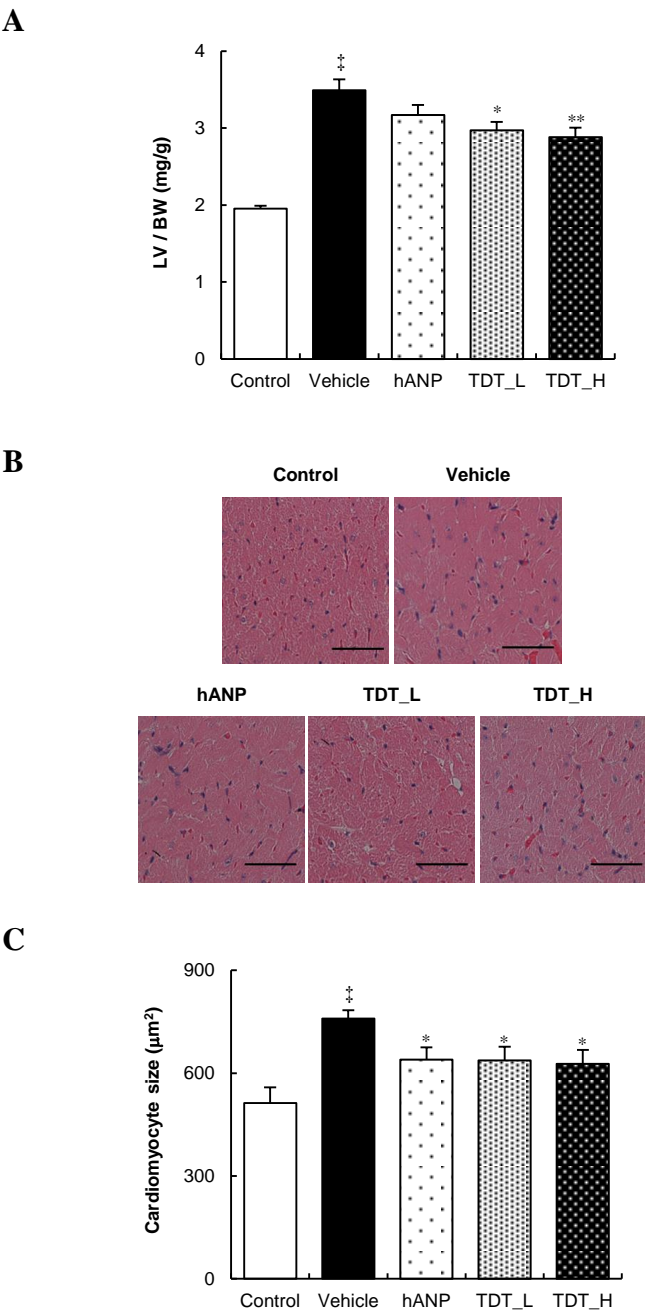
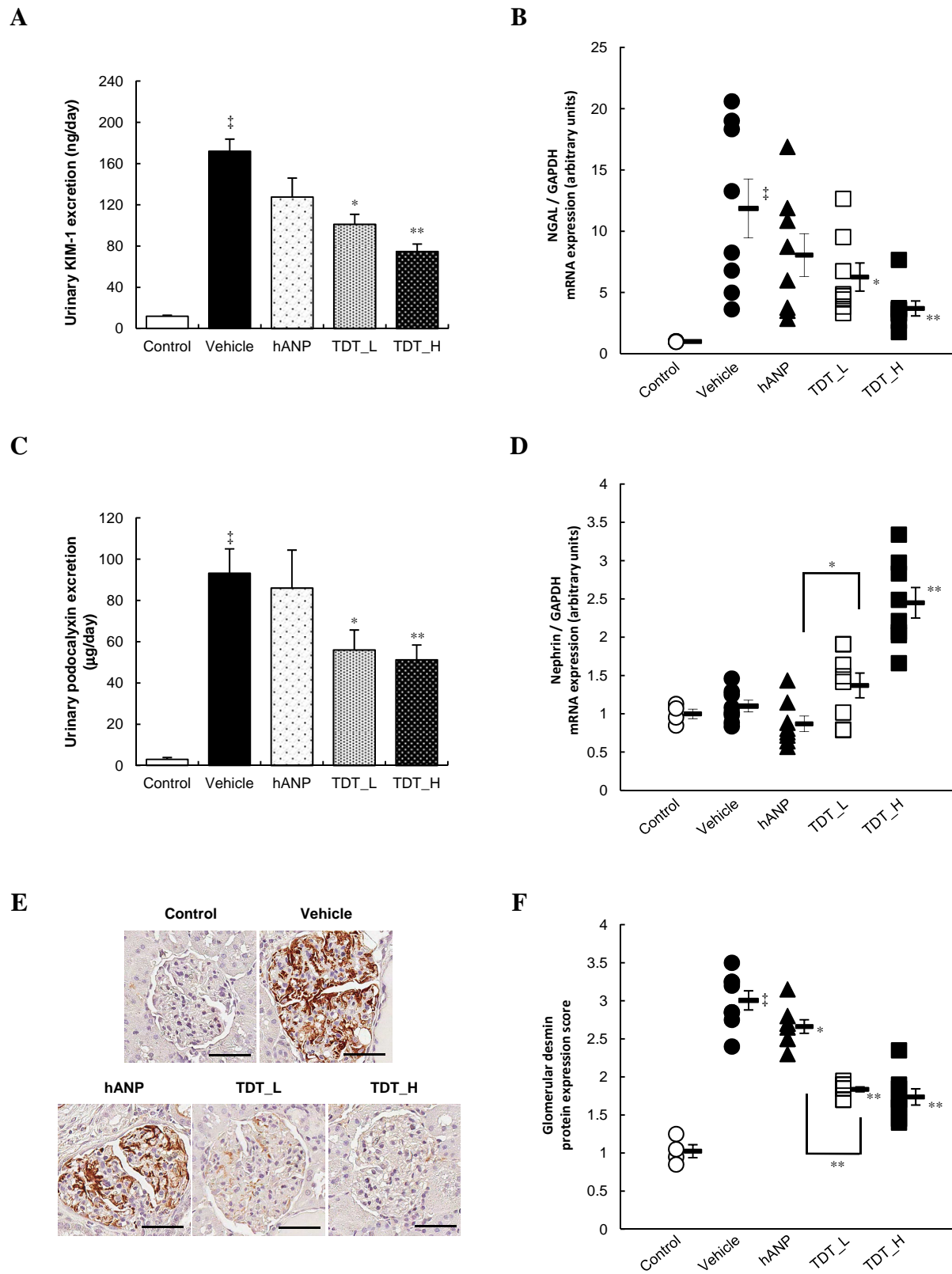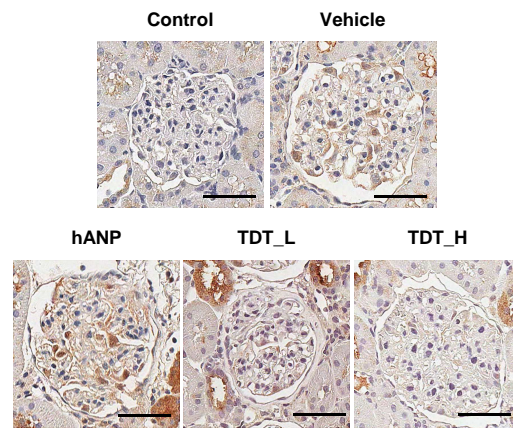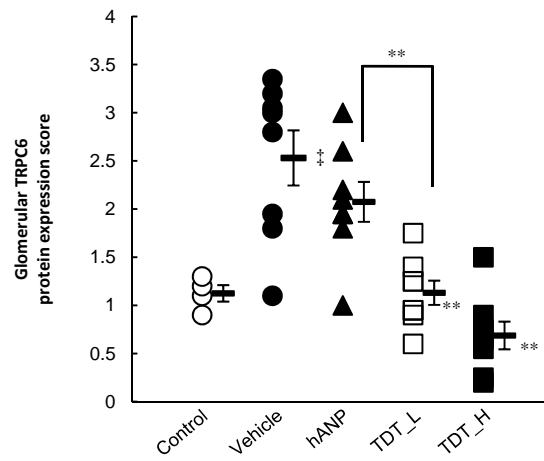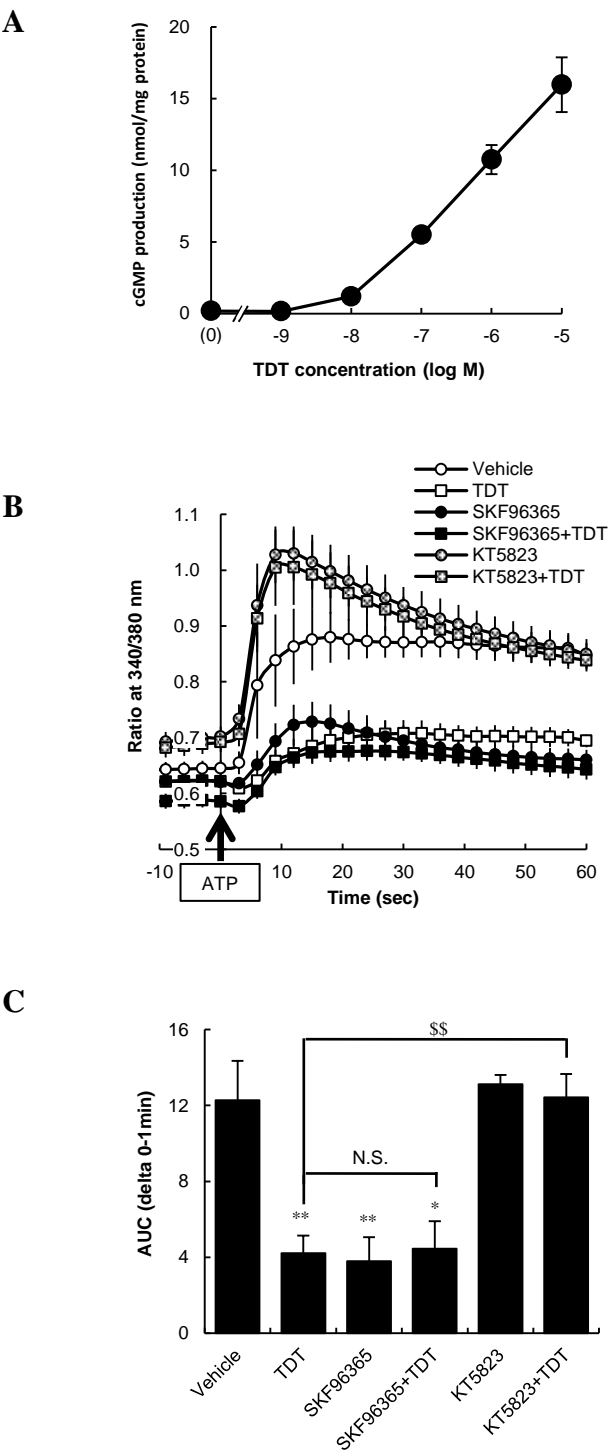**The Journal of Pharmacology and Experimental Therapeutics**

Sustained activation of guanylate cyclase-A with TDT, a natriuretic peptide derivative, exhibits cardiorenal protection in Dahl salt-sensitive hypertensive rats

Shohei Oishi, Naoko Suzuki, Yuri Hasui, Tsuyoshi Homma, Masanori Obana, Takahiro Nagayama, Yasushi Fujio

Laboratory of Clinical Science and Biomedicine, Graduate School of Pharmaceutical Sciences, Osaka University, Osaka, Japan (S.O., M.O., Y.F.)

End-Organ Disease Laboratories, Daiichi Sankyo Co., Ltd, Tokyo, Japan (S.O., Y.H., T.H.)

Rare Disease & LCM Laboratories, Daiichi Sankyo Co., Ltd, Tokyo, Japan (T.N.)

Research Function, Daiichi Sankyo Co., Ltd, Tokyo, Japan (N.S.)
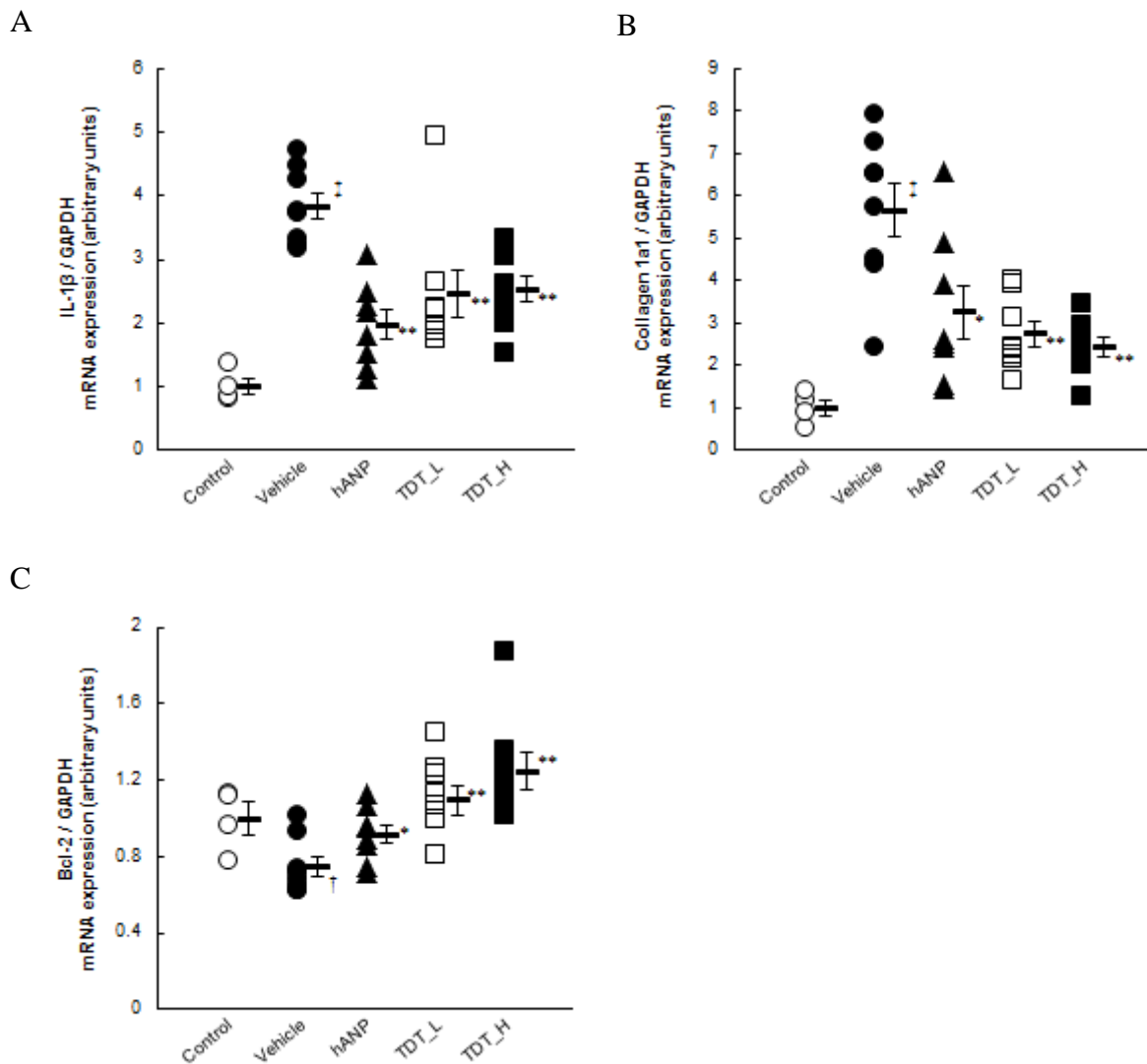
Address correspondence to:

Yasushi Fujio

Laboratory of Clinical Science and Biomedicine, Graduate School of Pharmaceutical Sciences, Osaka University, Osaka, Japan

1-6 Yamadaoka, Suita, Osaka, 565-0871, Japan

Tel.: +81 6 6879 8258; fax: +81 6 6879 8253

E-mail: fujio@phs.osaka-u.ac.jp

Supplemental Figure

A

B

C

Supplemental Fig. TDT and hANP modulated mRNA expression of IL-1β, collagen 1a1, and bcl-2 in kidney.

mRNA expression of IL-1β, collagen 1a1, and bcl-2 was determined by real-time quantitative PCR in DS rat kidneys at 20 weeks of age and normalized to that of GAPDH mRNA level (n = 4 for Control, n = 8 for the other groups). Data are presented as the mean ± S.E.M. [†] $P < 0.05$, [‡] $P < 0.01$ vs. Control, [*] $P < 0.05$, [**] $P < 0.01$ vs. Vehicle.